Cohesive laws x-fem association for simulation of damage fracture transition and tensile shear switch in dynamic crack propagation.

Alain Combescure, Michel Coret, Thomas Elguedj, Fabien Cazes, David Haboussa

Available online at www.sciencedirect.com

SciVerse ScienceDirect

Procedia IUTAM 3 (2012) 274 – 291

Procedia IUTAM

www.elsevier.com/locate/procedia

Cohesive laws X-FEM association for simulation of damage fracture transition and tensile shear switch in dynamic crack propagation.

Alain Combescure[a*], Michel Coret[a], Thomas Elguedj[a], Fabien Cazes[a], David Haboussa[a b]

[a] *Universite de lyon, INSA de Lyon, LaMCoS UMR CNRS 5256 18-20 allée des sciences 69621 Villeurbanne Cedex (France)*
[b] *DCNS / CSB Rue Choiseul, Porte Colbert, 56100, Lorient, (France)*

Abstract

This paper is devoted to the formulation of transitions in fracture for quasi static and dynamic crack propagation. It is organized in three parts. The first one describes a general way to construct a cohesive law which is thermodynamically equivalent to a damaging bulk material. The second part is devoted to the proposition of a unique dynamic crack propagation law which discriminates between tensile and shear cracking in case of moderate plasticity at crack tip. The third part of the paper compares experiments with simulation in both cases.

Keywords: crack initiation, cohesive law, crack propagation, X-FEM

1. Introduction

This paper summarizes a number of recent results obtained for crack propagation simulation. It is mainly devoted to the numerical treatment of switches and transition between different formulations of the same problem. The usual strategy is to use a unique formulation to simulate the whole damaging process. The standard practice is to use damage mechanics for fracture simulation of an initially undamaged object. These methods suffer from artificial localization but these defects are well known and a number of remedies have been proposed and are now rather well mastered: they all rest on the idea of non locality of damage [1][2][3][4][5]. Other methods are specialized for the simulation of propagation of existing cracks: this type of research have recently had a fast development essentially because of the appearance of X-FEM technologies [6][7]which ensured efficient and reliable predictions with e relatively coarse mesh.

 doi:10.1016/j.piutam.2012.03.017

The method was developed first for quasi static analysis and further for transient dynamic cases [8][9]. This paper proposes a method to link the two approaches.

One first develops and implement a damage to fracture transition model. These ideas pioneered by Mazars and Comi [10][11] are developed and implemented in the X-FEM cohesive framework [12][13]. This part shows how a cohesive law fully consistent with the damaging bulk material law can be developed and implemented.

One then gives a new analytical evaluation of crack propagation angle in case of shear fracture. It is then explained how this criterion can be combined with a tensile fracture criterion, to get an unique crack propagation angle valid for all situations.

Finally some examples are given to illustrate the concepts: these simulations are compared to experimental results.

Nomenclature

c	sound speed
c_R	Raighley wave speed
h	finite element size
l_c	characteristic damage length
τ_c	characteristic time for controlled damage rate model.
D	damage
σ	stress
ε	strain
$\Delta\sigma$	measure of the amplitude of stress wave
σ_{crit}	critical stress state
E	Young's modulus
L	Bar length
ΔL	Bar elongation
$[\![u]\!]$	Displacement jump in the cohesive element
σ^s	Cohesive normal stress
G	Applied energy release rate
G_C	Critical energy release rate
K_I	Mode I stress intensity factor
K_{II}	Mode II stress intensity factor

$\underline{\underline{\tilde{\sigma}}}$	Mean stress tensor ahead of crack tip
$\tilde{\sigma}*$	Measure of the intensity of this mean stress
$\tilde{\sigma}_{22}$	Stress normal to crack direction at crack tip
$\tilde{\sigma}_{12}$	Shear stress at crack tip
θ_c^{hoop}	Crack propagation angle for hoop stress criterion (brittle case)
θ_c^{shear}	Crack propagation angle for shear fracture criterion
ε_p^{hoop}	Cumulated plastic strain under which crack propagates in brittle mode
ε_p^{shear}	Cumulated plastic strain over which crack propagates in shear mode
$\dot{a}$	Crack tip velocity

2. Damage to fracture transition

2.1. Damage models and localization control

One considers an elastic or elasto-plastic material which is subjected to damage. The main difficulty associated with the use of damage models in numerical simulation is the artificial localization which can be controlled by the use of non local models: this approach imposes that damage spreads in a zone whose characteristic length is l_c: it follows from that observation that if the size h of the finite elements is smaller than $l_c/2$ the computation is no longer mesh dependant: this concept is nevertheless heavy to use in transient impact computation and heavy to implement. In dynamics the use of controlled damage rate models (cite allix deu) is often preferred. It consists to introduce a characteristic time τ_c such that the maximum damage rate $\dot{D}_c$ is limited to $1/\tau_c$. This model is physically reasonable as it ensured that the porosities cannot grow at an infinite rate. One can show [14] in 1D that these models are equivalent and that the localization length l_c is linked the to characteristic time τ_c by the following equation:

$$l_c = \frac{c}{\tau_c} \log\left(\frac{\Delta\sigma}{\sigma_{crit}}\right) \qquad (1)$$

In equation (1) c is the sound speed $\Delta\sigma$ is the amplitude of the stress wave and σ_{crit} a critical stress (for instance the cohesive stress). One may observe that this model supposes that the stress wave is larger than the critical stress (which is natural because if the applied stress is sub critical no damage can occur). One shall now observe that the damage representation of fracture have the drawback to impose very refined numerical models and that they reach their limit when large crack propagation are modeled.

2.2. A three scale model for fracture: from damage localization to large propagating cracks

Hence one would like to switch from damage to cohesive zone when it is appropriate and later to fracture in order to have efficient crack propagation models. In some sense one may see this approach as a three scale model. A fine scale for which damage is considered to be continuous, a meso scale, for which the damaging zone is represented by a cohesive law, and finally a coarse macroscopic scale occurring when the crack has reached a sufficient length for which standard fracture mechanics concept can be applied. Figure 1 underneath summarizes the proposed approach:

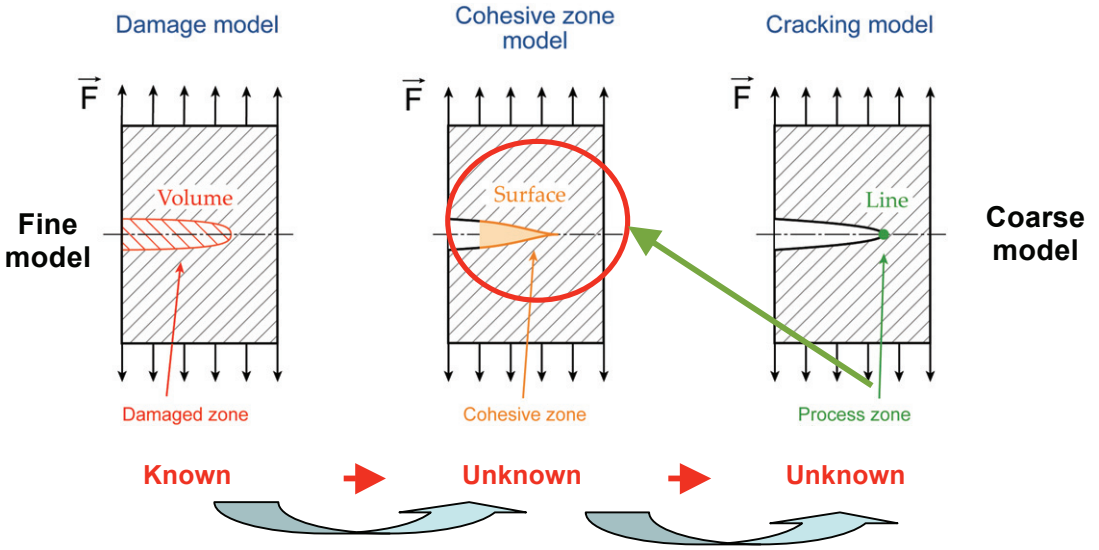

Fig. 1. The three "scales" used to describe damage to fracture transition

2.3. From damage to cohesive law

This section is devoted to the transition between damage model to cohesive zone model. One must now indicate that the method proposed here does not take into account the micro structure (grains adhesive joints, ect…) which may be of great importance in the damage to fracture transition. To pass from a 3D (resp. 2D) damaged volume (resp. surface) to a 2D (reps. 1D) cohesive zone one will use the following very simple concept: the rate of dissipated energy up to rupture will be the same in the volume (resp. surface) as on the corresponding cohesive surface (rep. line). This concept can be found in Bazant

[2] , Mazars and Pijaudier Cabot [10]. It has been used and developed to the concept of cohesive laws later by Cazes [15]. Figure 2 illustrates the concept:

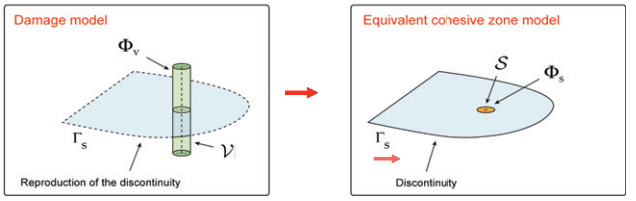

$$\Phi_s = \int_l \Phi_v \, dl$$

Fig. 2. The damage to cohesive zone transition

Let us observes that one must define the height of the "tube" with base S. This length is usually chosen as four time the damage characteristic length l_c or larger: this ensures that no localization of damage is totally included in the change of scale. One can then use this concept to construct incrementally a cohesive law which is perfectly equivalent to the damaging material and which dissipates exactly the same energy as the damage progresses into the material. This procedure is described in details in Cazes1 for elastic damaging materials. One could wonder which is this necessary as one is able to compute the damaging material laws. The main limitation of the pure damage approach is that the computation becomes heavy to handle and often unstable when the damaged zone becomes large. Some authors simply remove the damaged elements: this procedure works but must be handled with great care: one one side if the element is removed before the damage has reached the value 1. some uncontrolled elastic energy is removed from the mesh when one removes the element. Moreover in case of dynamic analysis one often removes nodes with the elements which also removes a part on kinetic energy from the system. One hence can deduce from that analysis that there are problems of energy control in such simulations. One shall now detail a bit further the main ideas to obtain a cohesive law completely equivalent to the damage material.

2.4. Elastic damage case

The following figure 3 summarizes one change of scale for an elastic damaging material.

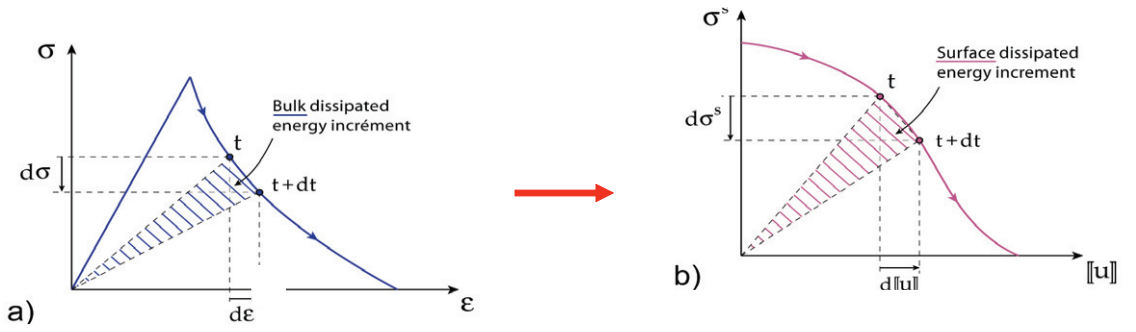

$$d\Phi_v = \frac{1}{2}\left(\sigma \, d\varepsilon - \varepsilon \, d\sigma\right) \quad = \quad d\Phi_s = \frac{1}{2}\left(\sigma^s \, d[\![u]\!] - [\![u]\!] \, d\sigma^s\right)$$

Fig. 3. a) continuous 1D stress strain law. b) corresponding cohesive law.

One computes a 1D elastic damaging bar including the preferred "non local" damage limiter. This produces a stress strain curve law (figure 3a). One replaces the damaged zone by a 1D cohesive segment which has a 1D cohesive law. Considering that the rate of dissipated energy in the bulk is the same as the surface dissipation energy rate, one constructs incrementally step by step the corresponding cohesive law given in figure 3b. This curve gives the cohesive normal stress σ_n as a function of the interface normal displacement jump $[\![u]\!]$. One must observe here that this change of scale model relies on two underlying hypothesis for the basic model: the first one is the definition of a characteristic length l_c. Following figure 4 gives the identification for a simple Mazars elastic damage model.

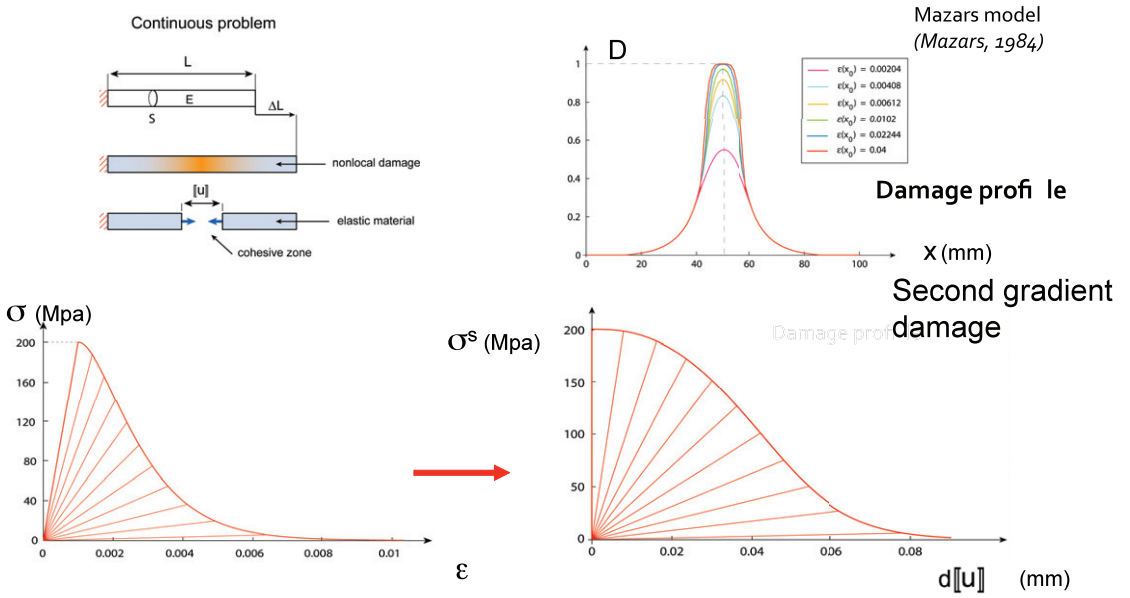

Fig. 4 construction of cohesive law from Mazars elastic damage model. Left damage model stress strain law. Right corresponding cohesive law.

The identification is easily done in 1D, but with such model the effects of variable triaxialities is not obvious to take into account. One may use a cylindrical 1D bar to take into account a constant controlled triaxiality. This type one 1D cylindrical bar model can also handle large strains effects in a simplified manner.

2.5. Elasto plastic case

The same type of approach can be developed for elastoplastic damaging materials [16]. One has then to identify the elastic as well as the plastic part of the dissipated energy in the bulk and t transfer these quantities on the cohesive laws. These two constraints allow to define the two parts of the elastoplastic cohesive laws. This is illustrated in the following figure 5.

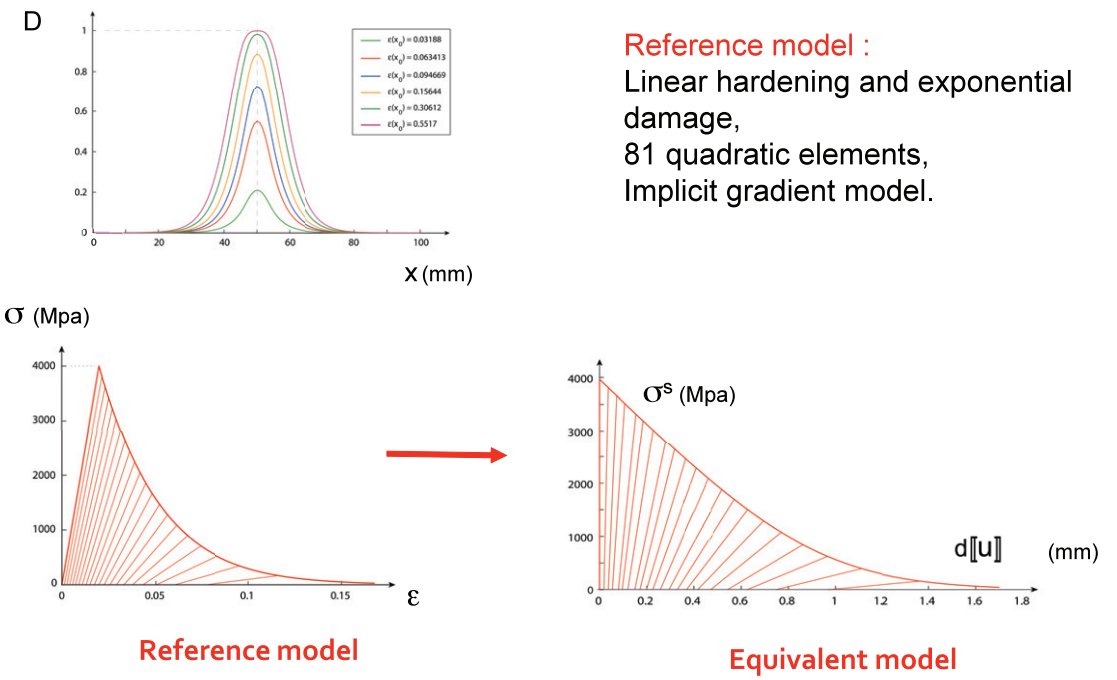

Fig. 5 construction of cohesive law from linear hardening elastoplastic associated with exponential damage model. Left damage model stress strain law. Right corresponding cohesive law.

2.6. Damage cohesive elements switch

Once the consistent cohesive model has been built one must introduce it within the computation at the right instant. Two procedures can be followed.

The first one relies on pure cohesive view of fracture modeling. When the critical state is reached (e. g. the critical stress at element interface) the following procedure is followed:

1) the nodes of the corresponding interface are doubled.

2) A cohesive element is inserted with the ad hoc cohesive law and the internal variables of the cohesive elements are initiated at zero.

3) The computation goes on with the extra nodes.

In case of dynamic analysis the mass matrix is recomputed when nodes are doubled.

The second approach is based on X-FEM and level sets. The proposed procedure now consists in the following steps:

1) compute the damage model incrementally in a standard manner

2) check the stability of the material for each Gauss point in each element using an appropriate criterion (e. g. loss of ellipticity of the tangent stress strain operator, of critical damage reached…)

3) when stability is lost in one element, add jump degree of freedom, update the level sets function to advance the discontinuity line by one element. The direction of the birthing crack direction is chosen accordingly to the direction found in step 2. The size of the new opening crack should be chosen in such a way that the new element is fully cracked. If there are more than one crack one can repeat the preceding strategy given for only one crack.

4) Initiate the cohesive points on the zero level set line using the previously defined cohesive law.

2.7. General comments

This model is suitable for the crack initiation stage and the early propagation one. Once the crack is long enough it is autonomous and its propagation is mainly driven by the "far" fields. The detailed crack tip material state is not of major importance for crack propagation laws. The region where damage and cohesive laws occur are denoted process zone in figure 1. The detailed material state and histories can be synthesized in a propagation law based on a "coarse" measure of the crack tip stress and strain state (e. g. the K_I K_{II} K_{III} stress intensities. The following section is dedicated to the development of such a method in case of competition between tensile and shears crack propagation.

3. A unique framework for tensile shear transition for 2D dynamic crack propagation with X-FEM

This section is devoted to the simulation of long crack propagation. One concentrates here on cases where there is a competition between two crack propagation modes: the first one is the classical tensile failure associated with the maximum hoop stress, whereas the second one is associated with shear driven fracture. One will first give the general strategy and then an analytical expression of tensile end shear crack propagation direction. One will then explain how one can model the crack choice of propagation direction.

3.1. General method

One now describes the simple model chosen to simulate this mode choice or transition. The following simplifying assumptions are done. The stress and strain state which drive the crack propagation is estimated with a mean value extracted from the stress field in a "small" region in a half disk "HD" ahead the crack tip; This disk radius should be larger than 3 elements size h: the following equation is used to extract the mean value $\tilde{x}$ of any quantity x:

$$\tilde{x} = \frac{\int_{HD} x(M) e^{-10\frac{d^2}{r^2}} dV}{\int_{HD} e^{-10\frac{d^2}{r^2}} dV} \qquad (2)$$

In equation (2) d is the distance between the crack tip and the point M within the disk where quantity x is evaluated and r is the radius of the half disk. This equation is used to defined a "mean" stress state $\tilde{\underline{\underline{\sigma}}}$ from which one can extract the desired quantities. The stress state is evaluated in a local frame tangent to the crack tip direction. The direction 1 is tangent to the crack tip and 2 is the normal one. The crack propagation criterion is the same if the crack propagates in shear or in tensile mode. This can be justified by the fact that a crack propagates when some measure of the "mean" stress at crack tip ($\tilde{\sigma}^*$) reaches the critical stress σ_{crit} . This criterion does not depend on propagation direction and is also valid in non linear elasticity. The second hypothesis is that the crack tip velocity $\dot{a}$ is not affected by the propagation mode (shear or tensile) and is given by the following Kaninnen phenomenological formula:

$$\dot{a} = c_R \left(1 - \frac{\sigma_{Crit}}{\tilde{\sigma}^*} \right) \tag{2}$$

Once the crack propagates and its velocity is known, one will look for its direction of propagation which depends of the stress intensities ratio. One can measure this ratio with two methods: the stress intensities K_I and K_{II} or a measure of the "local" stress state $\tilde{\underline{\underline{\sigma}}}$ ahead of crack tip. This paper shall concentrate on the second method to estimate the two intensities of the applied stress. One shall first recall the formula which gives the maximum hoop stress direction, then propose a new equation to predict the maximum shear stress propagation direction and finally explain how these criterion can be combined.

3.2. Maximum hoop stress crack propagation direction.

This direction θ_C^{hoop} is given by the following equation which is the translation of the standard formula in terms of local stress:

$$\theta_C^{Hoop} = 2 \arctan \left(\frac{1}{4} \left[\frac{\tilde{\sigma}_{22}}{\tilde{\sigma}_{12}} - sign\left(\tilde{\sigma}_{12}\right) \sqrt{2^3 + \left(\frac{\tilde{\sigma}_{22}}{\tilde{\sigma}_{12}} \right)^2} \right] \right) \tag{3}$$

3.3. Maximum shear stress crack propagation direction

There no available analytical expression for the propagation direction in case of shear driven propagation. The maximum shear direction has been derived by the authors from a numerical evaluation of the angle. An analytical fit is then proposed which gives the following formula for the estimation of the critical shear stress direction θ_C^{shear} :

$$\theta_C^{Shear} = sign\left(\tilde{\sigma}_{12}\right) \frac{\pi}{4} \arctan \left(0.186 \left[\left| \frac{\tilde{\sigma}_{22}}{\tilde{\sigma}_{12}} \right| + \sqrt{\frac{1}{3^3} + \left(\frac{\tilde{\sigma}_{22}}{\tilde{\sigma}_{12}} \right)^2} \right] \right) \tag{4}$$

One may observe that this equation is formally rather similar to the previous one.

3.4. Choice of appropriate direction

In case of competition between the two crack propagation mode one has to give an choice criterion to the crack. The experimental observation is that a crack which propagates in shear mode is usually a shear band associated with very localized high temperature increase. It was decided as this phenomenon is very fast which result in an adiabatic heat to simply use the elastoplastic strain around crack tip (which is proportional to heat input) to decide the type of propagation. A high strain at crack tip is associated with intense plastic dissipation and hence intense heating and shear driven cracking whereas a small strain is associated with tensile hoop stress failure. One has then choosen two equivalent plastic strains to decide the propagation angle. If the mean cumulated plastic strain ahead of crack tip (ε_p^*) is smaller than a value denoted ε_p^{hoop} the crack propagation angle is θ_C^{hoop}. If this strain measure is larger than ε_p^{shear}. In between a linear mixture rule is applied. Figure 6 explains the idea.

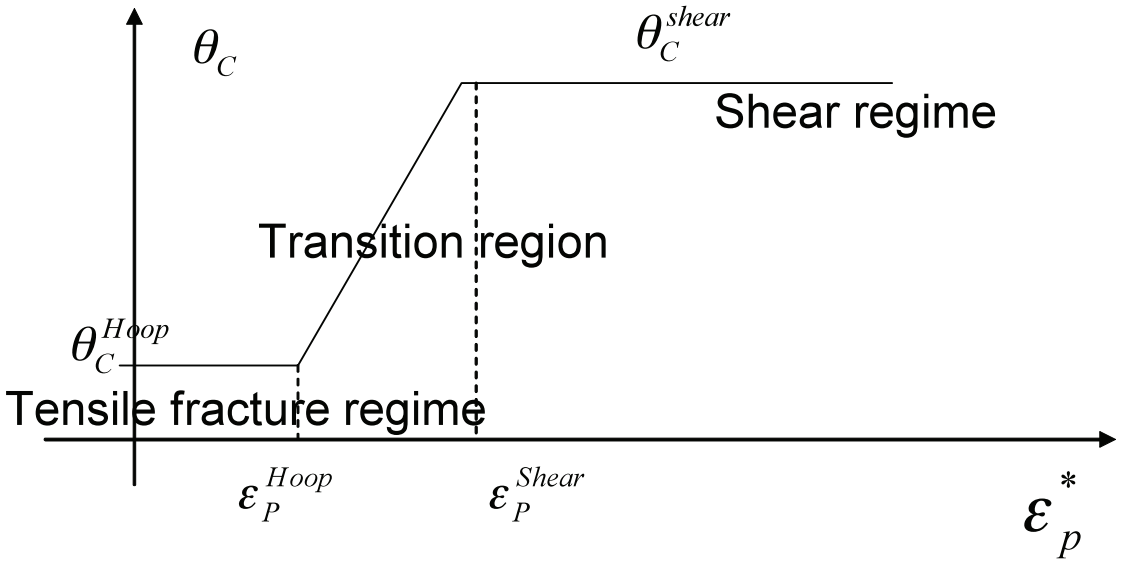

Fig. 6 Strategy to choose between tensile or shear crack propagation mode.

Let us observe that this concept relies on the definition of an equivalent plastic strain ahead crack tip. This is not an universal value: this number is the mean cumulated plastic strain in the HD region. The value is of course mesh and material dependant. But this is very difficult to avoid such considerations when one evaluates a strain ahead a moving stress in elasto-plasticity. Hence the value must be identified from experiments with a specific mesh size and then used as it is to predict other experiments, which must have the same mesh size. This is a limitation of the proposed method.

4. Two applications

Two examples shall be presented in this section: one for the transition from damage to cohesive zone, the second for shear tensile transition.

4.1. Static crack propagation with consistent cohesive model for 16MnD5 Steel

The elastoplastic cohesive zone model has been developed for the Rousselier's model [17] common to represent the nonlinear ductile damage model for 16MnD5 steel. It has been identified since a long time for all sorts of situations and temperatures. It is commonly used to simulate ductile crack propagation within the frame of classical damage mechanics. The main problem of this procedure is that it is limited to "small" crack propagation as nearly all simulations no longer converge after a propagation which is longer than some millimeters. This "divergence" is mainly due to excessive distortions of the "broken" elements. If these elements are removed the computation still does not converge because of the lack of control of removed energy with the element removal. The failure criterion is a critical porosity of the damaged material. For more details one can look at Simatos paper [18]. The cohesive zone model has first been constructed using the method described in section 2 and the resulting cohesive laws id given in the following figure 7

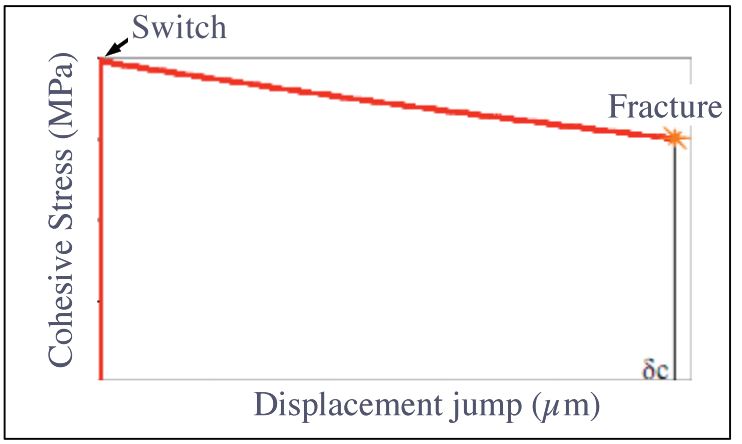

Fig. 7 Cohesive law consistent with Rousseilier's model for 16MnD5 ferritic steel.

One this model is identified a CT20 grooved test with long propagation is simulated in plane strain. The specimen is displayed in figure 8. The X-FEM finite element mesh is given in figure 9. It has about 3000 linear 4 nodes elements: most of them are standard 4 node elements and about 200 elements are X-

FEM 4 nodes elements, with only jump discontinuous elements. These elements are subdivised in 16 sub elements having each 4 gauss points.

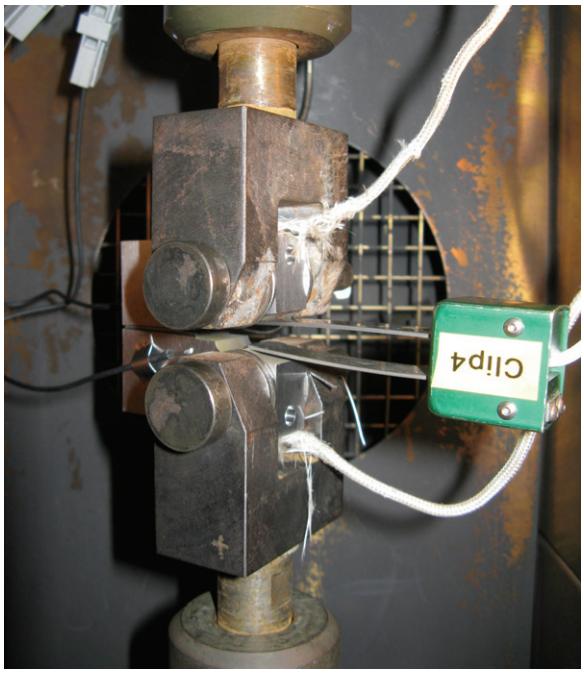

Fig. 8 : Photo of the test on CT20 groove specimen

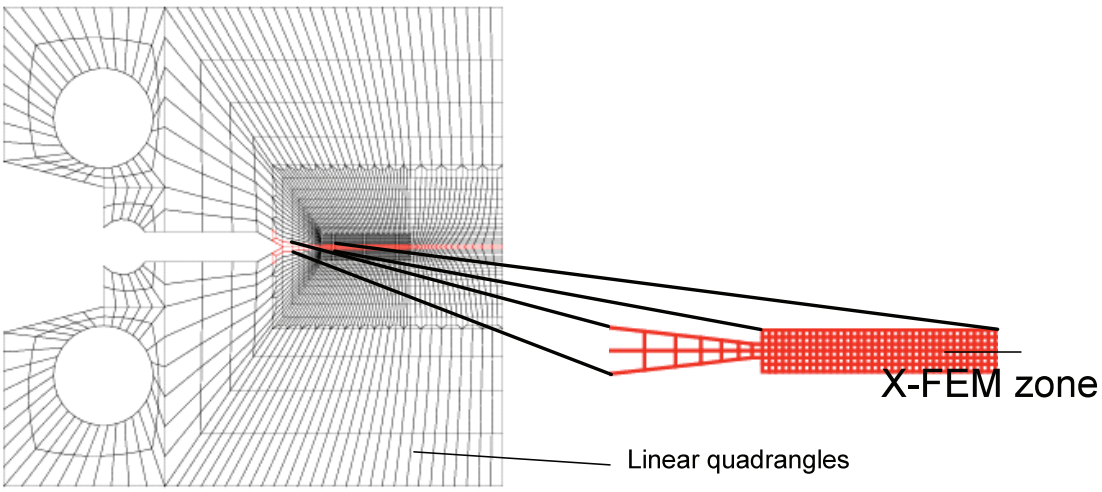

Fig. 9: Mesh for the computation

The computation is performed in elastoplasticity with the X-FEM level set method explained in section 2. The crack propagation angle is here zero because of the symmetries and the presence of groove. Figure 10 compares the result of the crack propagation computation obtained by the method of damage to cohesive method switch with the results obtained with standard damage model.

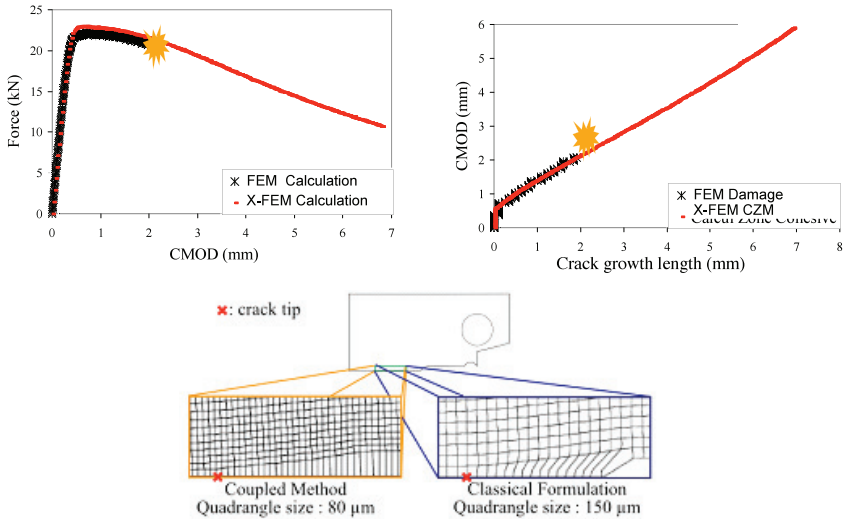

Fig. 10: comparison of Cohesive-XFEM predictions with standard damage modeling of crack propagation (CMOD= crack mouth opening displacements)

One clearly observes that the new method which switches from damage to cohesive law permits much longer crack propagation. The observation of the deformed mesh after 2mm propagation shows the reason of this difference: excessive distortion of the elements close to the crack in case of damage modelisation. Figure 11 displays the comparison of computed CMOD with experimental measure. This comparison shows that the identified Rousselier's model coefficient are valid for a small propagation but should be re evaluated if one wants to handle a larger propagation.

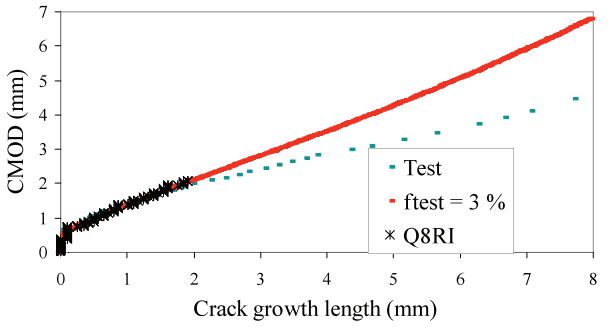

Fig. 11: Comparison of experimental CMOD with Cohesive-XFEM predictions as a function of crack length.

4.2. Interpretation of Zhou Rosakis Ravishandran switch crack propagation experiment.

The experiment is described in details in [19]. It has been modeled using extremely fine meshes and refined models for shear band formation by some authors [20] [21] [22][23]. The experiments consist in sending a mass on a cracked specimen. If the velocity of the impactor is higher than a critical value V_C the crack propagates approximately in a horizontal direction: this direction is consistent with a shear driven crack propagation process. When the impactor velocity is under V_C the crack starts to propagate horizontally and suddenly changes direction, when it reaches the half of the ligament: the new direction makes an angle of approximately 60° with the horizontal direction. Let us observe that the first direction is the direction associated to the shear propagation direction and that the second one corresponds to the direction associated with a pure mode II tensile hoop. The transition velocity is very sharp. The material used here is a high resistance maraging steel. Figure 12 shows a sketch of the experiment.

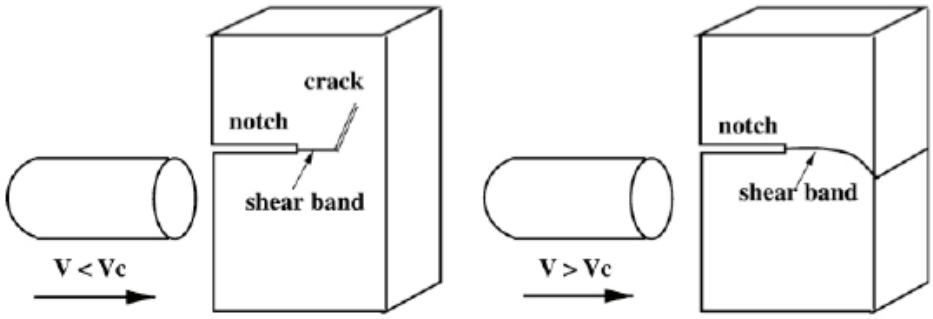

Fig. 12: Zhou Rosakis Ravishandran's experiment

The experiment is computed with the model described in section 3. The specimen is meshed with about 2000 4 node X-FEM elements. The computation is done with explicit code Europlexus [24] (cite Europlexus) and the lumped mass matrix technique given by Menouillard [25]. The following material parameters have been identified for the model and the chosen mesh size: Young's modulus 199000MPa, Poisson's ratio 0.3, density 8000, linear hardening isotropic plasticity model with Yield stress 190MPa and tangent modulus of 1600MPa, the critical stress is chosen to be 100MPa the two characteristic strains are $\varepsilon_p^{hoop} = 0.00675$ and $\varepsilon_p^{shear} = 0.00840$. The value of the yield stress as well as critical stress are much smaller than expected. This is due to the choice of a coarse mesh for the simulation which does not permit to "see" the large stresses at crack tip as well as the very thin shear band zone which characterize this type of shear crack propagation. Two computations are presented: the first one with an impactor velocity of 25 ms^{-1}, the second with an impactor velocity of 31 ms^{-1}. Figure 13 (resp. 14) displays the crack path for impact velocity of 25 ms^{-1} (resp. 31 ms^{-1}).

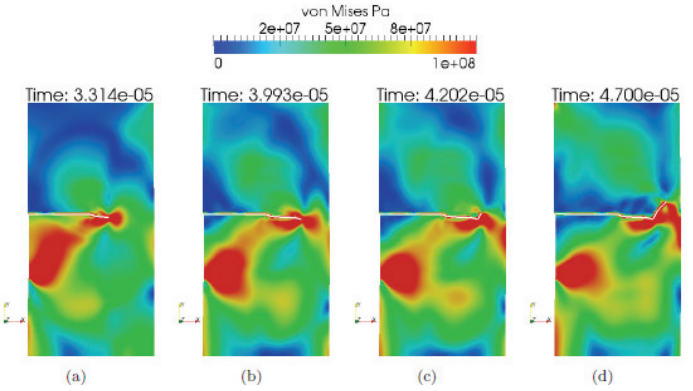

Fig. 13: Computation result for 25m S^{-1} impact velocity

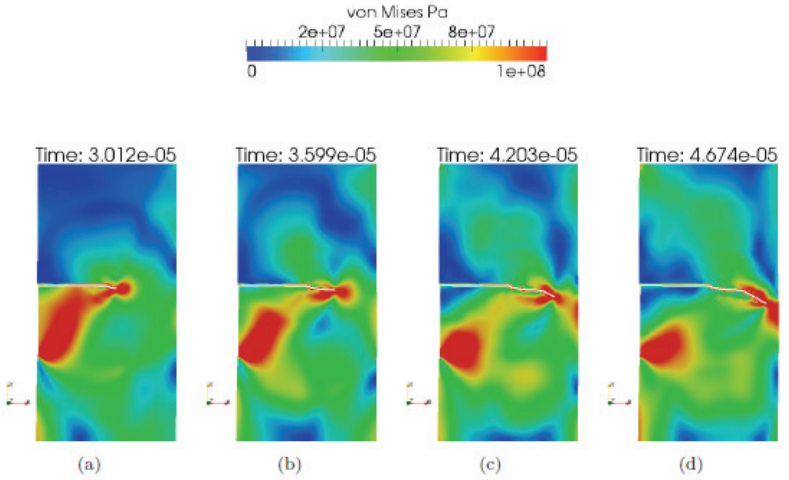

Fig. 14: Computation result for 31m S^{-1} impact velocity

One clearly observes the experimental result: the crack changes direction in case of slow impact velocity and not in case of high velocity. The transition between these two regimes is very sharp as in the experiments. Figure 15 shows the paths obtained with various impact speed which clearly confirm this experimental observation.

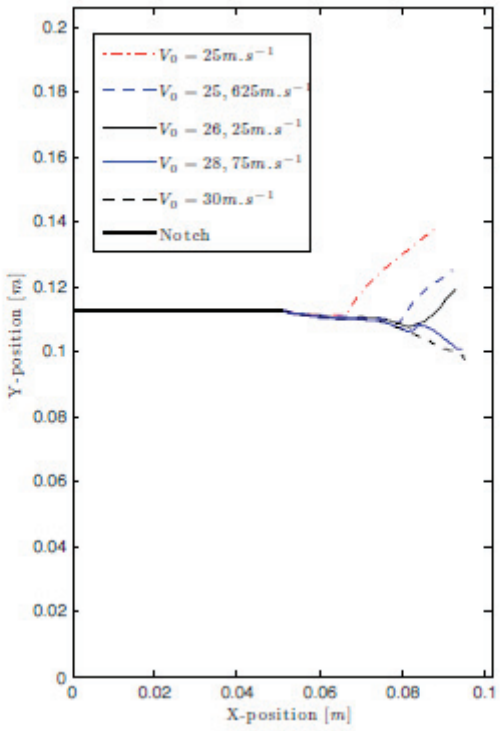

Fig. 15: Effect of impact velocity of crack path.

5. Conclusion

This paper has described the new research results on fracture mode transitions obtained by the research team. In quasi static it was shown how one can handle in a controlled manner the switch from a damaging model to a cohesive representation of fracture in the early stage of propagation. This work remains to be extended for 3D applications for which the proposed method should be really more efficient than the pure damage approach. It should also be extended to dynamic cases. The second switch between shear and tensile dynamic fracture mode seem to give "good" results although the proposed method relies on a very (too?) simple model of shear crack propagation. The idea remains to be tested on a large number of tests and to be extended to 3D cases. This method nevertheless requires a parameter identification which is mesh and material dependant.

Acknowledgements

These works have been supported by SAFRAN company as well as by DCNS. CEA has supported the work giving free use of Europlexus Code.

References

[1] Rice J, The localisation of plastic deformation, in : W Koiter, editor . *Theoretical and applied mechanics*; p 207-220.

[2] Pijaudier-Cabot G., Bazant Z., Non local damage theory. *Journal of engineering mechanics,* 1987;**113**: p 1512-1533.

[3] de Borst R., Mulhauss H. B., Gradient dependant plasticity: formulation and algorithmic aspects, *International journal of numerical methods and engibeering, 1992*;**35,**:p 521-539.

[4] Peerling R., de Borst R., Brekelman W., de Vree J., Gradient enhanced damage for quasi brittle materials, *International journal of numerical methods and engibeering, 1996*;**39,**:p 3391-3403.

[5] de Borst R., Pamin J, Geers M., On coupled Gradient-dependant plasticity and damge theories with a view to localization anlysis, *European journal of mechanics (A) solids, 1999*;**18,**:p 939-962.

[6] Moes N., Dolbow J., Belytschko T., A finite element method for crack growth without remeshing, *International journal of numerical methods and engibeering, 1999*;**46,**:p 131-150.

[7] Fries T., Belytschko T., The extended generalized finite element method: an overview of the method and its applications, *International journal of numerical methods and engibeering, 2010*;**84-3,**:p 253-304.

[8] R.ethore J, Gravouil A., Combescure A., An energy-conserving scheme for dynamic crack growth using the extended finite element method., *International journal of numerical methods and engibeering, 2005*;**63,**:p 631-659.

[9] Menouillard T, Rethore J, Combescure A, Bung H, Efficient explicit time stepping for the extended finite element method., *International journal of numerical methods and engibeering, 2008*;**68,**:p 11-31.

[10] Mazars J., Pijuadier Cabot G., From damage to fracture mechanics and conversly: a combined approach. *International journal of solids and structures, 1996*;**33,**:p 3327-3342.

[11] Comi C., Perego H., Fracture based bi-dissipative damage model for concrete, *International journal of solids and structures, 2001*;**38,**:p 6427-6454.

[12] Ortiz M.., Pandolfi A.., Finite-deformation irreversible cohesive elements for three-dimensional crack-propagation analysis, *International Journal For Numerical Methods In Engineering, 1999,* **44(9),** p 1267--1282.

[13] Moës,N. , Belytschko, T., Extended finite element method for cohesive crack growth" *Engineering Fracture Mechanics*, 2002, **69(7),** p 813--833.

[14] Suffis A., Lubrecht A., Combescure A., Damage model with delay effects: analytical and numerical study of the characteristic damage length, *International journal of solids and structures, 2003*;**40,**;p 3463-3476.

[15] Cazes,F.., Coret M.., Combescure A.., Gravouil A., A thermodynamic method for the construction of a cohesive law from a nonlocal damage model, *International Journal of Solids and Structures*, 2009, **46(6),** p ,1476--1490.

[16] Cazes F., Simatos, A.., Coret M.., Combescure A., A cohesive zone model which is energetically equivalent to a gradient-enhanced coupled damage-plasticity model, *European Journal of Mechanics - A/Solids ,* 2010, in Press

[17] Rousselier,G., Ductile fracture models and their potential in local approach of fracture, *Nuclear Engineering and Design* 1987, 105, p 97-111

[18] Simatos A., Cazes F. Marie S, Combescure A., Modeling ductile tearing from diffuse plasticity to crack propagation, 2010, *PVP paper 2010-25387*Cazes F., Simatos, A.., Coret M.., Combescure A., A cohesive zone model which is energetically equivalent to a gradient-enhanced coupled damage-plasticity model, *European Journal of Mechanics - A/Solids ,* 2010, in Press

[19] Zhou M, Rosakis A.J, Ravichandran G., Dynamically propagating shear bands in impact-loaded prenotched platesÑI. Experimental investigations of temperature signatures and propagation speed*., Journal of the Mechanics and Physics of Solids*,1996, **44**, p 981--1006.

[20] Zhou M, Rosakis A.J, Ravichandran G., Dynamically propagating shear bands in impact-loaded prenotched platesÑII. numerical simulations, *Journal of the Mechanics and Physics of Solids*, 1996,, **44,** p 1007--1032.

[21] Li S, Liu W.K, Rosakis A.J, Belytschko T, Hao W., Mesh-free Galerkin simulations of dynamic shear band propagation and failure mode transition, *International journal of Solids and Structures,* 2002, **67**, p 868--893.

[22] Song J.H, Areias P.M.A, Belytschko T., A method for dynamic crack and shear band propagation with phantom nodes, *International Journal for Numerical Methods in Engineering*, 2006**, 67**, p 868--893.

[23] Armero J.H, Linder C., Numerical simulation of dynamic fracture using finite elements with embedded discontinuities, *International Journal of Fracture*, 2009, **160**, p. 119--141.

[24] Europlexus web page.http://europlexus.jrc.ec.europa.eu/March, 2010

[25] Menouillard T, Rethore J, Moes N, Combescure A, Bung H., Mass lumping strategies for X-FEM explicit dynamics : Application to crack propagation., *International Journal for Numerical Methods in Engineering*, 2008, **74-3**, p 447--474.